World Journal of Gastroenterology

ORIGINAL ARTICLE

Basic Study

Protective effects of *Foeniculum vulgare* root bark extract against carbon tetrachloride-induced hepatic fibrosis in mice

Cai Zhang, Xing Tian, Ke Zhang, Guo-Yu Li, Hang-Yu Wang, Jin-Hui Wang

Cai Zhang, Xing Tian, Ke Zhang, Guo-Yu Li, Hang-Yu Wang, Jin-Hui Wang, School of Pharmacy, Shihezi University, Shihezi 832002, Xinjiang Uygur Autonomous Region, China

Abstract

AIM

To investigate the protective effects of *Foeniculum vulgare* root bark (FVRB), a traditional Uyghur medicine, against carbon tetrachloride (CCl4)-induced hepatic fibrosis in mice.

METHODS

Mice were randomly divided into eight groups (n = 20 each). Except for the normal control group, mice in the rest groups were intraperitoneally injected (i.p.) with 0.1% CCl4-olive oil mixture at 10 mL/kg twice a week to induce liver fibrosis. After 4 wk, mice were treated concurrently with the 70% ethanol extract of FVRB (88, 176, 352 and 704 mg/kg, respectively) daily by oral gavage for 4 wk to evaluate its protective effects. Serum aspartate aminotransferase (AST), alanine aminotransferase (ALT), triglyceride (TG), hexadecenoic acid (HA), laminin (LN), glutathione (GSH), superoxide dismutase (SOD), and malondialdehyde (MDA) in liver tissues were measured. Hematoxylin-eosin (H and E) staining and Masson trichrome (MT) staining were performed to assess histopathological changes in the liver. The expression of transforming growth factor β_1 (TGF-β_1), matrix metalloprotein 9 (MMP-9) and metallopeptidase inhibitor 1 (TIMP-1) was detected by immunohistochemical analysis. Additionally, TGF-β_1 and alpha-smooth muscle actin (α-SMA) protein expression was measured by Western blot.

RESULTS

A significant reduction in serum levels of AST, ALT, TG, HA and LN was observed in the FVRB-treated groups, suggesting that FVRB displayed hepatoprotective effects. Also, the depletion of GSH, SOD, and MDA accumulation in liver tissues was suppressed by FVRB. The expression of TGF-β_1, MMP-9 and TIMP-1 determined by immunohistochemistry was markedly reduced in a dose-dependent manner by FVRB treatment. Furthermore, protective effects of FVRB against CCl$_4$-induced liver injury were confirmed by histopathological studies. Protein expression of TGF-β_1 and α-SMA detected by Western blot was decreased by FVRB treatment.

CONCLUSION

Our results indicate that FVRB may be a promising agent against hepatic fibrosis and its possible mechanisms are inhibiting lipid peroxidation and reducing collagen formation in liver tissue of liver fibrosis mice.

Core tip: Hepatic fibrosis is a wound-healing pathological process resulting from chronic hepatic injuries. In the present study, hepatoprotective effects of *Foeniculum vulgare* root bark (FVRB), a traditional Uyghur medicine, against carbon tetrachloride (CCl$_4$)-induced hepatic fibrosis in mice were investigated. FVRB reduced serum levels of aspartate aminotransferase, alanine aminotransferase, triglyceride, hexadecenoic acid and laminin. Furthermore, FVRB inhibited CCl$_4$-induced TGF-β_1, MMP-9, TIMP-1 expression and histopathological changes. Our study indicated that the protective effects of FVRB are through inhibiting lipid peroxidation and collagen formation in liver tissue of liver fibrosis mice.

INTRODUCTION

Hepatic fibrosis is a wound-healing pathological process resulting from chronic hepatic injuries, which is characterized by the accumulation of extracellular matrix (ECM)[1]. It occurs during most continuous and chronic liver diseases, driven by inflammatory responses to tissue injury, which ultimately lead to liver cirrhosis. Previous studies indicated that activation of hepatic stellate cells (HSCs) plays an important role in the progress of hepatic fibrosis[2,3]. Activation of HSCs increases cell proliferation, producing large amounts of ECM components including hexadecenoic acid (HA) and laminin (LN)[4,5]. In addition, aberrant activity of transforming growth factor β_1 (TGF-β_1) or members of the platelet derived growth factor family are also the most prominent drivers to activate and transdifferent HSCs into myofibroblast[6,7]. Further, several chemokines that modulate the inflammatory reaction are involved in the progression of HSC activation and the fibrotic insult[8,9]. Many studies have demonstrated that the reversion of fibrosis can be achieved, particularly in the early course of the disease. Currently, treatment of liver damage mainly consists of inhibiting early activation and proliferation of HSCs and collagen fiber growth, and promoting HSC apoptosis and collagen degradation.

Many studies indicated that *Foeniculum vulgare* root bark (FVRB), a traditional Uyghur medicine, contains many chemical constituents, such as saccharides, glycosides, lactone compounds, phenols, tannins, flavonoids, alkaloids, volatile oil, grease, triterpenes and sterols[10,11]. In addition, FVRB has been traditionally used for the treatment of several pathophysiological conditions in China, exhibiting the activity of dispelling coldness, warming kidney and stomach, removing dampness, and alleviating swelling and pain[12-15]. For the first time, the present study was aimed to investigate the protective effects of FVRB against CCl$_4$-induced liver injury *in vivo* and the possible mechanisms involved.

MATERIALS AND METHODS

Animals

Male Kunming mice weighing 20 ± 2 g were supplied by the Experimental Animal Center of Urumqi (Urumqi, China). Mice were housed at room temperature under a 12 h light/dark cycle (lights on at 08:00 h) and were fed a standard diet *ad libitum*. All animal care and experimental procedures were approved by the Institute Ethnics Committee of Shihezi University.

Drug material

FVRB was obtained from Uygur Pharmaceutical Company (Uygur, China). FVRB was extracted with 70% ethanol by using the method of heating reflux and steam drying. A voucher specimen (No. 20070820) has been deposited in School of Pharmacy, Shihezi University.

Reagents

CCl$_4$ was obtained from Tianjin Guangfu Science and Technology Development Co. (Tianjin, China). Yiganling Pian (batch number 150102044) containing 38.5 mg of *Silybum marianum* each piece was purchased from Shanxi Lijun Chinese Medicine Co. (Shanxi,

China). Alanine aminotransferase (ALT), aspartate aminotransferase (AST), triglyceride, malondialdehyde (MDA), reduced glutathione hormone (GSH), and superoxide dismutase (SOD) assay kits were all purchased from Nanjing Jiancheng (Nanjing, China). Hyaluronic acid (HA) and laminin (LN) assay kits were obtained from Xitang Co. (Shanghai, China). Rabbit primary antibodies against TGF-β_1, alpha-smooth muscle actin (α-SMA), matrix metalloprotein 9 (MMP-9), and metallopeptidase inhibitor 1 (TIMP-1), and horseradish peroxidase labeled secondary antibody were purchased from BOSTER (Wuhan, China).

Experimental protocol

Mice were randomly divided into eight groups (n = 20 each): A-H. Group A (normal control group) was allowed free access to water and food. In the other seven experimental groups (B-H), the mice were treated with CCl_4 (10 mL/kg, i.p.) in olive oil (1:1000, v/v), twice a week for eight weeks. Group B served as a solvent control group, in which mice were given olive oil at 10 mL/kg at the fifth week. Group C was a model group, in which mice were given water at 10 mL/kg at the fifth week. Groups D, E, F, and G were orally administered with FVRB (88, 176, 352 and 704 mg/kg, respectively) once daily from the fifth week for four weeks. Group H was a positive control group, in which mice were treated with Yiganling Pian (200 mg/kg).

Mice were anesthetized with ethyl ether and blood samples were harvested. The blood was centrifuged at 3500 rpm for 10 min at 4 ℃ to obtain the supernatant serum, which was stored at 80 ℃ until further use for biochemical analysis. Liver, spleen and kidney were dissected out and washed immediately with ice cold saline to weigh.

Biochemical analysis

Serum was collected as mentioned above. ALT, AST and TG were determined according to the manufacturer's protocols using a Microplate Reader Thermo 3001. The absorbance of ALT and AST reactions was read at 505 nm and the absorbance of TG reaction was read at 546 nm. The enzyme activity is calculated as U/L. HA and LN levels were determined by enzyme-linked immunosorbent assay using the commercial kits. The absorbance of the reaction was read at 450 nm.

Measurement of MDA, GSH and SOD activities

Liver tissues samples were homogenized in physiological saline to give a 10% (w/v) liver homogenate, which was then centrifuged at 2500 rpm for 15 min at 4 ℃. The supernatant was used for the measurement of MDA, GSH and SOD activities with the commercial kits following the manufacture's protocols. Data are expressed as U/mg of protein.

Histopathological evaluation

Liver specimens were fixed in 10% formalin and then embedded in paraffin. Four-micrometer-thick sections were obtained from paraffin blocks and stained with hematoxylin and eosin (H and E) and Masson's trichrome (MT) before they were examined under a light microscope. The images were randomly taken from ten fields under a light microscope (200 × magnification).

Immunohistochemistry

TGF-β_1, MMP-9 and TIMP-1 expression levels in the liver were measured by immunohistochemistry. The liver tissues were sectioned and incubated with rabbit anti-TGF-β_1 antibody (1:100), rabbit anti-MMP-9 antibody (1:100), and rabbit anti-TIMP-1 antibody (1:100). Then the slides were processed using an immunohistochemical staining kit. After that, the slides were counterstained with hematoxylin and mounted with a glycerin gel. In the negative control groups, the primary antibodies were replaced with PBS. The sections were observed under a microscope (Nikon 80i).

Western blot analysis

Total protein was extracted from the liver tissue and the protein concentration was determination by BCA method. The protein was separated by SDS-polyacrylamide gel electrophoresis, followed by transfer to PVDF membrane. The membranes were blocked with 5% nonfat milk in TBST buffer for 1 h. Then target proteins were incubated overnight at 4 ℃ with TGF-β_1 and α-SMA primary antibodies (1:1000). After washing four times with TBST, the membranes were incubated with HRP-conjugated secondary antibody (1:10000) for 1 h at room temperature. Then the membranes were immersed in an enhanced chemiluminescence detection solution. Protein was analyzed by the gray value of the band, which is expressed as the ratio of the target protein and the β-actin protein.

Statistical analysis

All quantitative data are expressed as mean ± SE. Data were analyzed with SPSS 13.0 software. Statistical significance between groups was determined by one-way analysis of variance (ANOVA) followed by Tukey's multiple range post hoc test. $P < 0.05$ was considered statistically significant.

RESULTS

Effect of FVRB on organ index increase induced by CCl_4 treatment

As demonstrated in Figure 1, organ indexes including liver, spleen and kidney coefficients were measured in mice. Similar to previous studies[16], liver and spleen indexes were significantly increased in mice treated with CCl_4. Compared with the model group, the increase of liver index and spleen index in CCl_4-treated group was reduced by FVRB and Yiganling Pian treatment. However, there were no significant
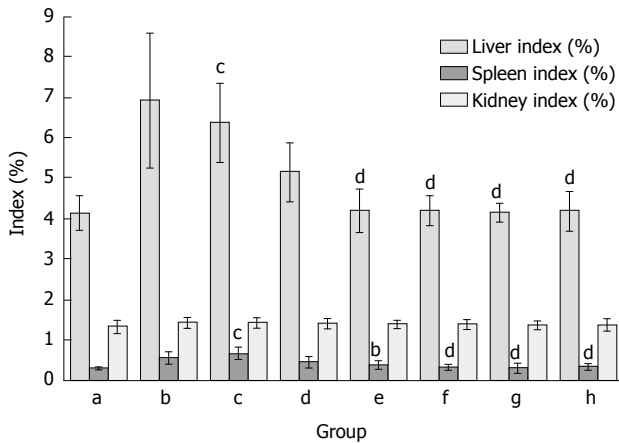
Figure 1 Effect of *Foeniculum vulgare* root bark extract on organ indexes in hepatic fibrosis mice. Data are expressed as the mean ± SD ($n = 20$). [b]P < 0.01 *vs* the normal control group; [c]P < 0.05 *vs* the CCl₄-treated group; [d]P < 0.01 *vs* the CCl₄-treated group. a: Normal group; b: Solvent group + CCl₄; c: CCl₄-treated group; d, e, f and g: FVRB treatment groups (88, 176, 352 and 704 mg/kg, respectively); h: Yiganling Pian + CCl₄.

Figure 2 Effect of *Foeniculum vulgare* root bark extract on alanine aminotransferase, aspartate aminotransferase and triglyceride activities in CCl₄-treated mice. Data are expressed as the mean ± SD ($n = 20$). [b]P < 0.01 *vs* the normal control group; [c]P < 0.05 *vs* the CCl₄-treated group; [d]P < 0.01 *vs* the CCl₄-treated group. a: Normal group; b: Solvent group + CCl₄; c: CCl₄-treated group; d, e, f and g: FVRB treatment groups (88, 176, 352 and 704 mg/kg, respectively); h: Yiganling Pian + CCl₄.

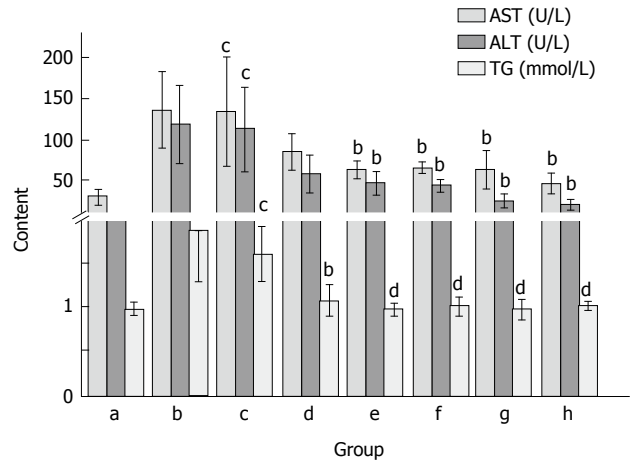differences in the kidney coefficient between the groups.

Effect of FVRB on serum AST, ALT and TG activities in mice

As shown in Figure 2, CCl₄ treatment markedly elevated serum AST, ALT and TG activities as compared with the normal control group. The AST and ALT activities after CCl₄ treatment were about 5 and 4 times higher than that of the normal group, respectively. However, Yiganling Pian treatment markedly inhibited the increase of serum AST, ALT and TG after long-term CCl₄ injection in mice (P < 0.05; Figure 2). Similarly, the administration of FVRB at different dosages significantly decreased AST, and ALT and TG activities (P < 0.05 or P < 0.01; Figure 2).

Effect of FVRB on MDA, GSH and SOD levels in CCl₄-treated mice

Lipid peroxidation was evaluated by measuring MDA content in liver tissue. In the CCl₄ treatment group, the content of MDA was elevated as compared with the normal control group. The administration of FVRB significantly decreased MDA content in a dose-dependent manner. Also, as compared with the normal control group, CCl₄ treatment markedly decreased the GSH level and SOD activity in liver tissue. However, treatment with the extract of FVRB (352 and 704 mg/kg) markedly recovered the CCl₄-induced GSH depletion (P < 0.01; Figure 3). In addition, FVRB treatment (88, 176, 352 and 704 mg/kg) significantly restored the depletion of SOD activity in a dose-dependent manner (Figure 3). Similarly, Yiganling Pian treatment (200 mg/kg) increased the GSH content and SOD activity as compared with the CCl₄ group (P < 0.01; Figure 3). Further, there was no significant difference in the levels of MDA, GSH and SOD between the CCl₄ group and the solvent control group.

Effect of FVRB on serum HA and LN in mice

After CCl₄ administration, the levels of serum HA and LN were significantly increased as compared with the normal control group (P < 0.05; Figure 4). Treatment with Yiganling Pian (200 mg/kg) significantly decreased the levels of serum HA and LN (P < 0.05; Figure 4). Meanwhile, FVRB treatment markedly decreased the elevation of serum HA and LN in a dose-dependent manner after long-term CCl₄ injection in mice (P < 0.05; Figure 4).

Effect of FVRB on histopathological alterations

As shown in Figure 5A, the liver sections of the normal control group exhibited the normal cellular structure with well-preserved cytoplasm, prominent nucleolus and central vein. In contrast, the liver sections of the CCl₄-treated group and solvent control group exhibited significant pathological changes, such as fibrosis, ballooning degeneration, steatosis, disseminated macrovesicular and microvesicular changes (Figure 5B and C). There was focal necrosis as well as piecemeal necrosis and fibrosis of portal areas. However, the FVRB and Yiganling Pian treatment groups showed a few to milder degree of leukocytes infiltration and necrosis (Figure 5E-H). In addition, as compared to the normal control group, the livers of mice treated with CCl₄ and the solvent exhibited extensive accumulation of connective tissue, leading to the formation of continuous fibrotic septa, nodules of regeneration, and noticeable alterations in the central vein (Figure 6A-C). However, treatment with FVRB and Yiganling Pian significantly attenuated CCl₄-induced alterations (Figure 6E-H). The severe hepatic fibrosis was reduced by treatment with FVRB, which was in good correlation with the results of hepatic antioxidant enzyme activities and serum aminotransferase activities.
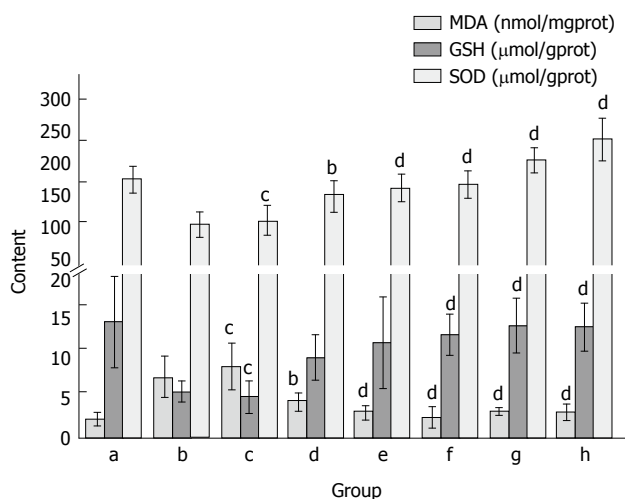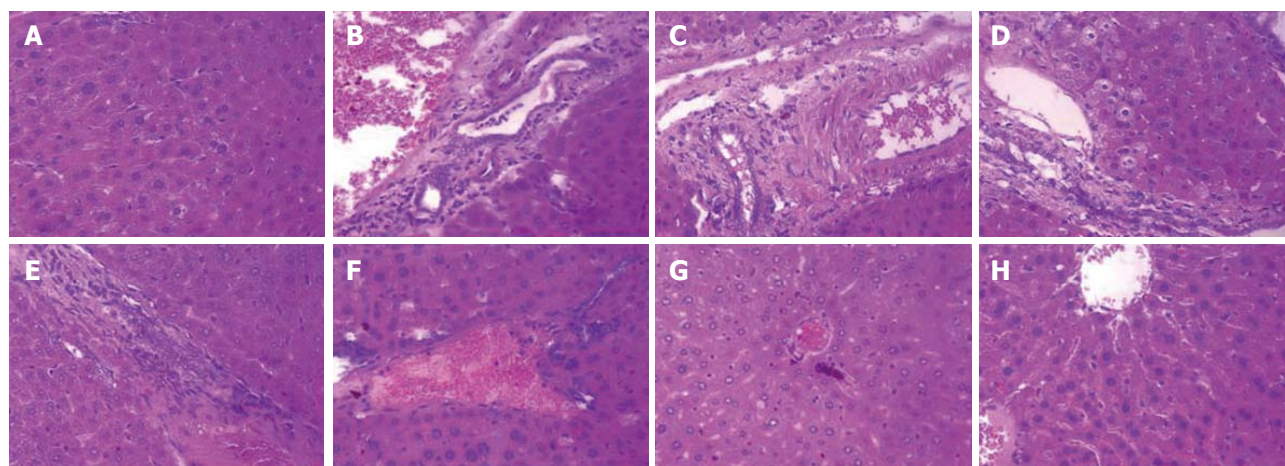
Figure 3 Effect of *Foeniculum vulgare* root bark extract on malondialdehyde, glutathione and superoxide dismutase levels in CCl₄-treated mice. Data are expressed as the mean ± SD ($n = 20$). [b]$P < 0.01$ *vs* the normal control group; [c]$P < 0.05$ *vs* the CCl₄-treated group; [d]$P < 0.01$ *vs* the CCl₄-treated group. a: Normal group; b: Solvent group + CCl₄; c: CCl₄-treated group; d, e, f and g: FVRB treatment groups (88, 176, 352 and 704 mg/kg, respectively); h: Yiganling Pian + CCl₄.
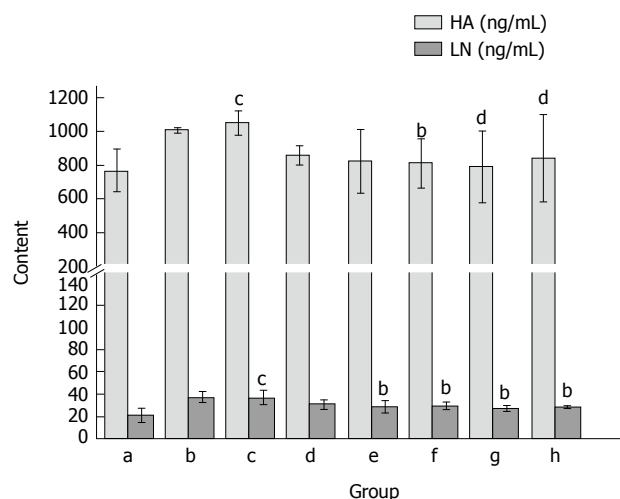
Figure 4 Effect of *Foeniculum vulgare* root bark extract on serum hexadecenoic acid and laminin levels in mice. Data are expressed as the mean ± SD ($n = 20$). [b]$P < 0.01$ *vs* the normal control group; [c]$P < 0.05$ *vs* the CCl₄-treated group; [d]$P < 0.01$ *vs* the CCl₄-treated group. a: Normal group; b: Solvent group + CCl₄; c: CCl₄-treated group; d, e, f and g: *Foeniculum vulgare* root bark (FVRB) treatment groups (88, 176, 352 and 704 mg/kg, respectively); h: Yiganling Pian + CCl₄.

Figure 5 H and E staining (× 400) of the liver sections of mice. A: Normal control group; B: Solvent group + CCl₄; C: CCl₄-treated group; D-G: *Foeniculum vulgare* root bark (FVRB) treatment groups (88, 176, 352 and 704 mg/kg, respectively); H: Yiganling Pian + CCl₄.

### Effect of FVRB on immunohistochemical staining for TGF-β₁, MMP-9 and TIMP-1

As shown in Figure 7A, the expression of TGF-β₁ in the normal control group was only observed in the portal area and central vein, with a relatively shallow, narrow range. In Figure 7B and C, the expression of TGF-β₁ in the model group was mainly distributed in the portal area and central vein, with brown granules showing a wide distribution. However, the positive expression of TGF-β₁ was significantly decreased in the FVRB treatment group (Figure 7D-G). The positive control group also showed a good reduction in the expression of TGF-β₁ (Figure 7H).

Immunohistochemical expression of MMP-9 protein is shown in Figure 8. Positive MMP-9 staining appeased as brown granules in the cytoplasm and membrane. The overall color of the normal group was light brown, while the model group was significantly different. Compared with the model group, the positive expression in the treatment group was decreased, especially in the dose group of 704 mg/kg.

The results of TIMP-1 protein expression are shown in Figure 9. In the normal control group, there was positive expression of TIMP-1 in peripheral blood vessels and bile duct wall of the portal area (Figure 9A). In the solvent group and the model group, the positive staining of TIMP-1 was distributed in the fiber spacing and the central vein, and the brown yellow was obviously visible (Figure 9B and C). Compared with the model group, the positive expression of TIMP-1 in the FVRB treatment groups was markedly decreased (Figure 9 D-G). Further, there was a small amount of
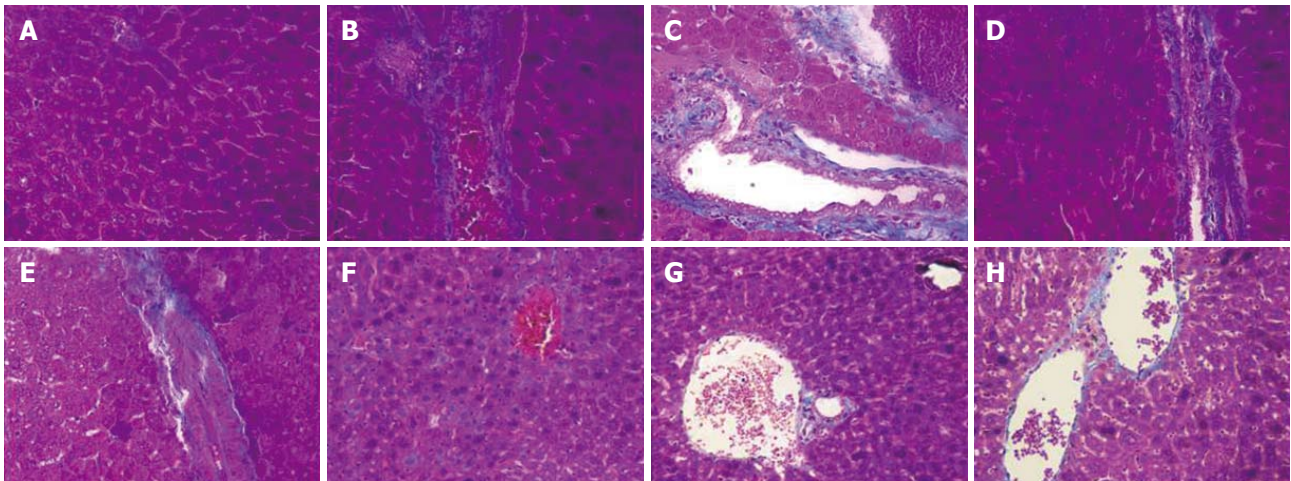
Figure 6 Masson trichrome staining (× 400) of the liver sections of mice. A: Normal control group; B: Solvent group + CCl₄; C: CCl₄-treated group; D-G: FVRB treatment groups (88, 176, 352and 704 mg/kg, respectively); H: Yiganling Pian + CCl₄.
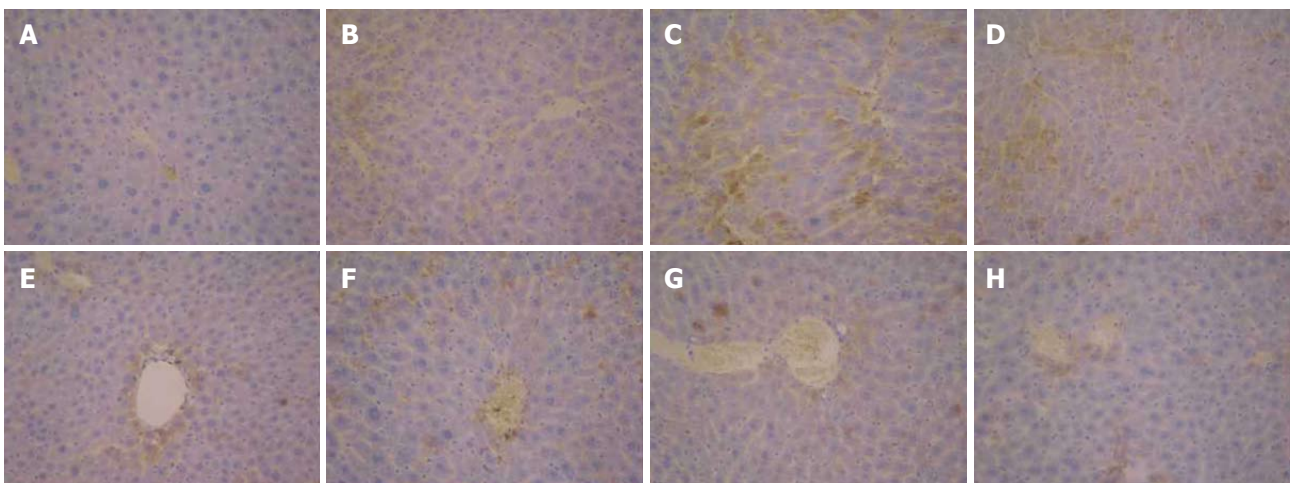
Figure 7 Immunohistochemical examination (× 400) of transforming growth factor β1 expression in liver tissues of mice. A: Normal group; B: Solvent group + CCl₄; c: CCl₄-treated group; D-G: *Foeniculum vulgare* root barks (FVRB) treatment groups (88, 176, 352 and 704 mg/kg, respectively); H: Yiganling Pian + CCl₄.
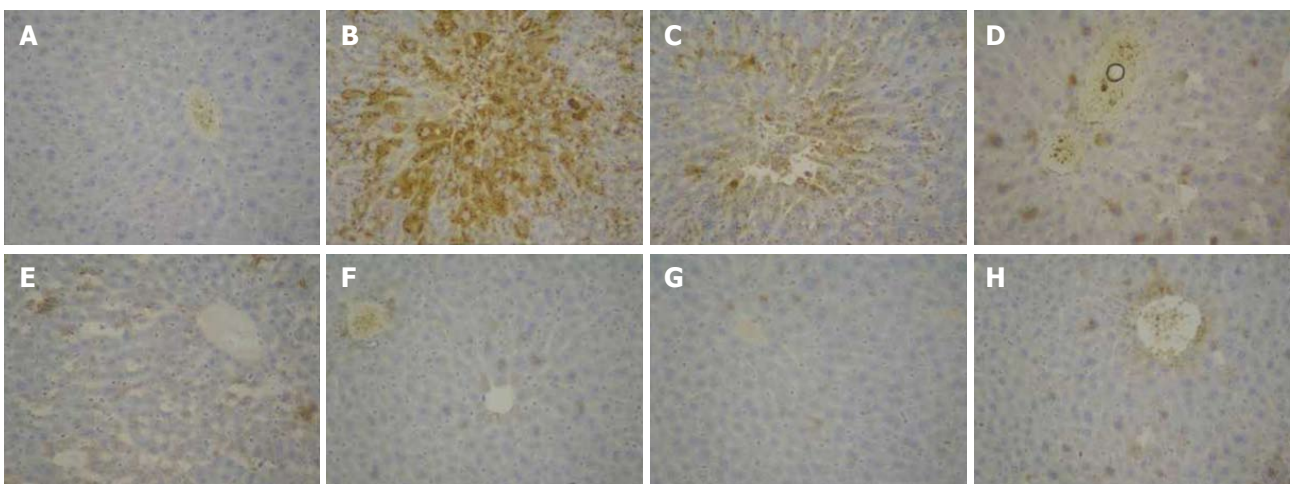
Figure 8 Immunohistochemical examination (× 400) of matrix metalloprotein 9 expression in liver tissues of mice. A: Normal control group; B: Solvent group + CCl₄; C: CCl₄-treated group; D-G: *Foeniculum vulgare* root bark (FVRB) treatment groups (88, 176, 352 and 704 mg/kg, respectively); H: Yiganling Pian + CCl₄.
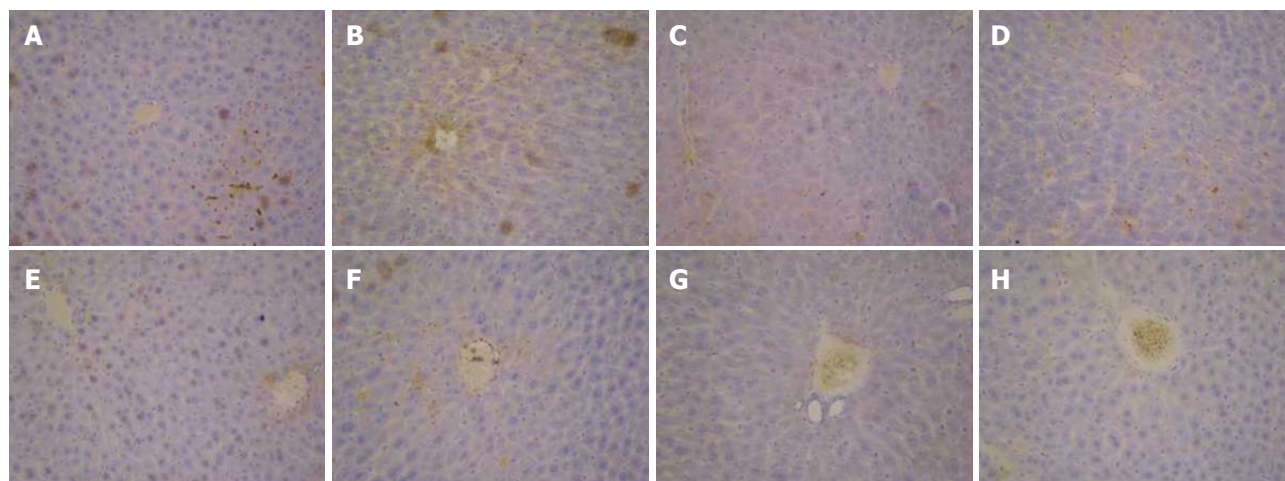
Figure 9 Immunohistochemical examination (× 400) of metallopeptidase inhibitor 1 expression in liver tissues of mice. A: Normal control group; B: Solvent group + CCl4; C: CCl4-treated group; D-G: *Foeniculum vulgare* root bark (FVRB) treatment groups (88, 176, 352 and 704 mg/kg, respectively); H: Yiganling Pian + CCl4.
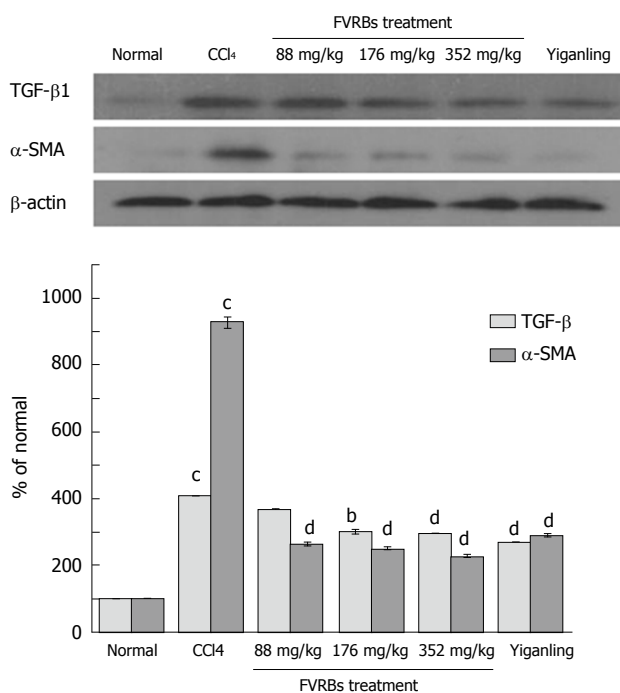

Figure 10 Effect of *Foeniculum vulgare* root bark extract on the expression of transforming growth factor-β1 and α-SMA proteins. [b]P < 0.01 *vs* the normal control group; [c]P < 0.05 *vs* the CCl4-treated group; [d]P < 0.01 *vs* the CCl4-treated group. TGF-β: Transforming growth factor β; α-SMA: Alpha-smooth muscle actin.

positive TIMP-1 staining in the Yiganling Pian positive control group (Figure 9H).

Effect of FVRB on TGF-β₁ and α-SMA protein expression

As illustrated in Figure 10, compared to the normal control group, the expression of TGF-β₁ and α-SMA in the CCl4 treatment group was significantly increased (*P* < 0.01). However, FVRB treatment markedly decreased TGF-β₁ and α-SMA expression as compared with the CCl4 treatment group (*P* < 0.05 or *P* < 0.01). Meanwhile, treatment with Yiganling Pian also significantly attenuated TGF-β₁ and α-SMA expression (*P* < 0.01).

DISCUSSION

Liver fibrosis is usually regarded as an outcome of chronic liver injury in the process of long-term wound healing[17-19]. In the present study, CCl4-induced liver injury, the most commonly used model for hepatic fibrosis[20,21], was induced. We detected the levels of ALT, AST, TG, HA and LN to assess liver function and the degree of liver fibrosis. There is evidence that natural substances may have a protective role against CCl4-induced liver injury[22,23]. Considerable efforts have been made in the study of natural products with hepatoprotective activities[24,25]. Our study showed that CCl4 caused a significant increase in serum levels of ALT, AST, TG, HA and LN in mice. However, FVRB treatment significantly altered these trends. Its hepatoprotective effect was further confirmed by histopathological observation that FVRB attenuated CCl4-induced necro-inflammatory and fibrogenic effects.

There is growing evidence that oxidative stress contributes to the development of liver fibrosis by activating various signaling pathways involved in fibrogenesis[26,27]. The tissue concentration of MDA, a product of lipid peroxidation during liver fibrogenesis, was assayed. Also, the SOD and GSH activities were measured. In the present study, in the CCl4-treated mice, the MDA level in liver tissue was elevated and the activities of SOD and GSH were decreased. Reversal of these trends by FVRB treatment suggests that FVRB prevented the progression of liver fibrosis by inhibiting oxidative stress in the liver.

The histopathological studies are a direct means for assessing the protective effect of FVRB. HE and Masson staining results showed that FVRB could reduce liver necrosis, significantly inhibit collagen fiber hyperplasia, improve liver tissue structure and reduce

fiber tissue. These results further confirmed that FVRB dose-dependently decreased hepatic histopathological changes.

The activation of HSCs is the central event in the pathogenesis of liver fibrosis[28-30]. In recent years, many studies found that TGF-β_1 is the strongest factor inducing fibrosis, and it is also an important factor to promote the activation of HSCs[28,31]. Our result confirmed that administration of FVRB reduced the expression of TGF-β_1 protein. Therefore, the anti-fibrotic effect of FVRB may be mediated by its inhibitory effect on TGF-β_1. In addition, α-SMA expression also increases the generation and proliferation of chemotactic factors that are capable of recruiting inflammatory cells[32,33]. From the results we know that expression of α-SMA was enhanced by CCl$_4$ treatment, while the administration of FVRB prevented the development of fibrosis perhaps through the inhibition of α-SMA.

The major pathological change of liver fibrosis is the excessive accumulation of collagen and other extracellular matrixes[34]. Under normal circumstances, the synthesis and decomposition of collagen is balanced. Once the synthesis is over than decomposition, it will cause the accumulation of collagen in the liver, leading to the formation of liver fibrosis[35]. Matrix metalloproteinases (MMPs) can promote the degradation of extracellular matrix, which is consistent with the previous finding that the tissue inhibitors of metalloproteinase (TIMPs) can reduce liver fibrosis severity[36,37]. Among the MMP family members, MMP-9 plays an essential role in fibrosis formation. Many studies have shown that MMP-9 is elevated in patients with liver fibrosis. TIMP-1 can inhibit MMP-9[38], preventing the degradation of ECM and thereby promoting liver fibrosis. In the present study, the expression of MMP-9 and TIMP-1 proteins showed significant differences between CCl$_4$ and FVRB treatment groups, which suggests that MMP-9 and TIMP-1 are related to the protective effects of FVRB against the formation of liver fibrosis.

In conclusion, FVRB dose-dependently ameliorated hepatic oxidative stress and suppressed inflammation in CCl$_4$-injured liver fibrosis, and its mechanisms against liver fibrosis may be related with inhibiting lipid peroxidation formation in liver tissue of liver fibrosis mice and reducing the collagen formation by suppressing protein expression of TGF-β_1, α-SMA, MMP-9 and TIMP-1. Thus, FVRB may have potential therapeutic utilities for protecting against liver fibrosis. Further experimental studies are necessary to determine the effective constituents of FVRB.

COMMENTS

Background
Hepatic fibrosis is a wound-healing pathological process resulting from chronic hepatic injuries, which is characterized by the accumulation of extracellular matrix. It occurs during most continuous and chronic liver diseases, driven by inflammatory responses to injury tissues, which ultimately lead to liver cirrhosis.

Research frontiers
Currently, treatment of liver damage mainly consists of inhibiting early activation and proliferation of hepatic stellate cells (HSCs) and collagen fiber growth, and promoting HSC apoptosis and collagen degradation. *Foeniculum vulgare* root bark (FVRB), a traditional Uyghur medicine, has been used for the treatment of several pathophysiological conditions in China, exhibiting the activity of dispelling coldness, warming kidney and stomach, removing dampness, and alleviating swelling and pain.

Innovations and breakthroughs
For the first time, the present study was aimed to investigate the protective effects of FVRB against CCl$_4$-induced liver injury *in vivo*. And its mechanisms against liver fibrosis may be related with inhibiting lipid peroxidation in liver tissue of liver fibrosis mice and inhibiting the collagen formation by suppressing protein expression of transforming growth factor-β_1, alpha-smooth muscle actin, matrix metalloprotein 9 and metallopeptidase inhibitor 1.

Applications
FVRB dose-dependently ameliorated hepatic oxidative stress and suppressed inflammation in CCl$_4$-injured liver injury. Thus, FVRB may have potential therapeutic utilities for protecting against liver fibrosis.

Terminology
Liver fibrosis is usually regarded as an outcome of chronic liver injury in the process of long-term wound healing.

Peer-review
The authors' aim was to investigate the protective effects of FVRB extract against carbon tetrachloride-induced hepatic fibrosis in mice. The methods are appropriate, and the results are moderate.

REFERENCES

1   **Iwakiri Y**, Shah V, Rockey DC. Vascular pathobiology in chronic liver disease and cirrhosis - current status and future directions. *J Hepatol* 2014; **61**: 912-924 [PMID: 24911462 DOI: 10.1016/j.jhep.2014.05.047]

2   **Tai CJ**, Choong CY, Lin YC, Shi YC, Tai CJ. The anti-hepatic fibrosis activity of ergosterol depended on upregulation of PPARgamma in HSC-T6 cells. *Food Funct* 2016; **7**: 1915-1923 [PMID: 27040153 DOI: 10.1039/c6fo00117c]

3   **Zhao J**, Tang N, Wu K, Dai W, Ye C, Shi J, Zhang J, Ning B, Zeng X, Lin Y. MiR-21 simultaneously regulates ERK1 signaling in HSC activation and hepatocyte EMT in hepatic fibrosis. *PLoS One* 2014; **9**: e108005 [PMID: 25303175 DOI: 10.1371/journal.pone.0108005]

4   **Mòdol T**, Brice N, Ruiz de Galarreta M, García Garzón A, Iraburu MJ, Martínez-Irujo JJ, López-Zabalza MJ. Fibronectin peptides as potential regulators of hepatic fibrosis through apoptosis of hepatic stellate cells. *J Cell Physiol* 2015; **230**: 546-553 [PMID: 24976518 DOI: 10.1002/jcp.24714]

5   **Thomas RG**, Moon MJ, Kim JH, Lee JH, Jeong YY. Effectiveness of Losartan-Loaded Hyaluronic Acid (HA) Micelles for the Reduction of Advanced Hepatic Fibrosis in C3H/HeN Mice Model. *PLoS One* 2015; **10**: e0145512 [PMID: 26714035 DOI: 10.1371/journal.pone.0145512]

6   **Peng J**, Li X, Feng Q, Chen L, Xu L, Hu Y. Anti-fibrotic effect of Cordyceps sinensis polysaccharide: Inhibiting HSC activation, TGF-β_1/Smad signalling, MMPs and TIMPs. *Exp Biol Med* (Maywood) 2013; **238**: 668-677 [PMID: 23918878 DOI: 10.1177/1535370213480741]

7   **He Y**, Huang C, Sun X, Long XR, Lv XW, Li J. MicroRNA-146a modulates TGF-beta1-induced hepatic stellate cell proliferation by targeting SMAD4. *Cell Signal* 2012; **24**: 1923-1930 [PMID: 22735812 DOI: 10.1016/j.cellsig.2012.06.003]

8   **Wasmuth HE**, Weiskirchen R. [Pathogenesis of liver fibrosis:

modulation of stellate cells by chemokines]. *Z Gastroenterol* 2010; **48**: 38-45 [PMID: 20072995 DOI: 10.1055/s-0028-1109933]

9   **Wasmuth HE**, Tacke F, Trautwein C. Chemokines in liver inflammation and fibrosis. *Semin Liver Dis* 2010; **30**: 215-225 [PMID: 20665374 DOI: 10.1055/s-0030-1255351]

10   **Parejo I**, Jauregui O, Sánchez-Rabaneda F, Viladomat F, Bastida J, Codina C. Separation and characterization of phenolic compounds in fennel (Foeniculum vulgare) using liquid chromatography-negative electrospray ionization tandem mass spectrometry. *J Agric Food Chem* 2004; **52**: 3679-3687 [PMID: 15186082 DOI: 10.1021/jf030813h]

11   **Badgujar SB**, Patel VV, Bandivdekar AH. Foeniculum vulgare Mill: a review of its botany, phytochemistry, pharmacology, contemporary application, and toxicology. *Biomed Res Int* 2014; **2014**: 842674 [PMID: 25162032 DOI: 10.1155/2014/842674]

12   **Tripathi P**, Tripathi R, Patel RK, Pancholi SS. Investigation of antimutagenic potential of Foeniculum vulgare essential oil on cyclophosphamide induced genotoxicity and oxidative stress in mice. *Drug Chem Toxicol* 2013; **36**: 35-41 [PMID: 22264205 DOI: 10.3109/01480545.2011.648328]

13   **Berrington D**, Lall N. Anticancer Activity of Certain Herbs and Spices on the Cervical Epithelial Carcinoma (HeLa) Cell Line. *Evid Based Complement Alternat Med* 2012; **2012**: 564927 [PMID: 22649474 DOI: 10.1155/2012/564927]

14   **Bogucka-Kocka A**, Smolarz HD, Kocki J. Apoptotic activities of ethanol extracts from some Apiaceae on human leukaemia cell lines. *Fitoterapia* 2008; **79**: 487-497 [PMID: 18672039 DOI: 10.1016/j.fitote.2008.07.002]

15   **Singh B**, Kale RK. Chemomodulatory action of Foeniculum vulgare (Fennel) on skin and forestomach papillomagenesis, enzymes associated with xenobiotic metabolism and antioxidant status in murine model system. *Food Chem Toxicol* 2008; **46**: 3842-3850 [PMID: 18976688 DOI: 10.1016/j.fct.2008.10.008]

16   **Tsai CF**, Hsu YW, Chen WK, Chang WH, Yen CC, Ho YC, Lu FJ. Hepatoprotective effect of electrolyzed reduced water against carbon tetrachloride-induced liver damage in mice. *Food Chem Toxicol* 2009; **47**: 2031-2036 [PMID: 19477216 DOI: 10.1016/j.fct.2009.05.021]

17   **Elpek GÖ**. Cellular and molecular mechanisms in the pathogenesis of liver fibrosis: An update. *World J Gastroenterol* 2014; **20**: 7260-7276 [PMID: 24966597 DOI: 10.3748/wjg.v20.i23.7260]

18   **Getachew Y**, Cusimano FA, Gopal P, Reisman SA, Shay JW. The Synthetic Triterpenoid RTA 405 (CDDO-EA) Halts Progression of Liver Fibrosis and Reduces Hepatocellular Carcinoma Size Resulting in Increased Survival in an Experimental Model of Chronic Liver Injury. *Toxicol Sci* 2016; **149**: 111-120 [PMID: 26443840 DOI: 10.1093/toxsci/kfv213]

19   **Melino M**, Gadd VL, Alexander KA, Beattie L, Lineburg KE, Martinez M, Teal B, Le Texier L, Irvine KM, Miller GC, Boyle GM, Hill GR, Clouston AD, Powell EE, MacDonald KP. Spatiotemporal Characterization of the Cellular and Molecular Contributors to Liver Fibrosis in a Murine Hepatotoxic-Injury Model. *Am J Pathol* 2016; **186**: 524-538 [PMID: 26762581 DOI: 10.1016/j.ajpath.2015.10.029]

20   **Huang SS**, Chen DZ, Wu H, Chen RC, Du SJ, Dong JJ, Liang G, Xu LM, Wang XD, Yang YP, Yu ZP, Feng WK, Chen YP. Cannabinoid receptors are involved in the protective effect of a novel curcumin derivative C66 against CCl4-induced liver fibrosis. *Eur J Pharmacol* 2016; **779**: 22-30 [PMID: 26945822 DOI: 10.1016/j.ejphar.2016.02.067]

21   **Hafez MM**, Hamed SS, El-Khadragy MF, Hassan ZK, Al Rejaie SS, Sayed-Ahmed MM, Al-Harbi NO, Al-Hosaini KA, Al-Harbi MM, Alhoshani AR, Al-Shabanah OA, Alsharari SD. Effect of ginseng extract on the TGF-β1 signaling pathway in CCl4-induced liver fibrosis in rats. *BMC Complement Altern Med* 2017; **17**: 45 [PMID: 28086769 DOI: 10.1186/s12906-016-1507-0]

22   **Sun Y**, Jia L, Huang Z, Wang J, Lu J, Li J. Hepatoprotective effect against CCl4-induced acute liver damage in mice and High-performance liquid chromatography mass spectrometric method for analysis of the constituents of extract of Rubus crataegifolius.

Nat Prod Res 2017; Epub ahead of print [PMID: 28322066 DOI: 10.1080/14786419.2017.1292264]

23   **Pareek A**, Godavarthi A, Issarani R, Nagori BP. Antioxidant and hepatoprotective activity of Fagonia schweinfurthii (Hadidi) Hadidi extract in carbon tetrachloride induced hepatotoxicity in HepG2 cell line and rats. *J Ethnopharmacol* 2013; **150**: 973-981 [PMID: 24140589 DOI: 10.1016/j.jep.2013.09.048]

24   **Vladimir-Knežević S**, Cvijanović O, Blažeković B, Kindl M, Štefan MB, Domitrović R. Hepatoprotective effects of Micromeria croatica ethanolic extract against CCl4-induced liver injury in mice. *BMC Complement Altern Med* 2015; **15**: 233 [PMID: 26174335 DOI: 10.1186/s12906-015-0763-8]

25   **Wahid A**, Hamed AN, Eltahir HM, Abouzied MM. Hepatoprotective activity of ethanolic extract of Salix subserrata against CCl4-induced chronic hepatotoxicity in rats. *BMC Complement Altern Med* 2016; **16**: 263 [PMID: 27473536 DOI: 10.1186/s12906-016-1238-2]

26   **Heeba GH**, Mahmoud ME. Therapeutic potential of morin against liver fibrosis in rats: modulation of oxidative stress, cytokine production and nuclear factor kappa B. *Environ Toxicol Pharmacol* 2014; **37**: 662-671 [PMID: 24583409 DOI: 10.1016/j.etap.2014.01.026]

27   **Domitrović R**, Jakovac H, Marchesi VV, Blažeković B. Resolution of liver fibrosis by isoquinoline alkaloid berberine in CCl4-intoxicated mice is mediated by suppression of oxidative stress and upregulation of MMP-2 expression. *J Med Food* 2013; **16**: 518-528 [PMID: 23734997 DOI: 10.1089/jmf.2012.0175]

28   **He YH**, Li Z, Ni MM, Zhang XY, Li MF, Meng XM, Huang C, Li J. Cryptolepine derivative-6h inhibits liver fibrosis in TGF-β1-induced HSC-T6 cells by targeting the Shh pathway. *Can J Physiol Pharmacol* 2016; **94**: 987-995 [PMID: 27295431 DOI: 10.1139/cjpp-2016-0157]

29   **Wang Q**, Dai X, Yang W, Wang H, Zhao H, Yang F, Yang Y, Li J, Lv X. Caffeine protects against alcohol-induced liver fibrosis by dampening the cAMP/PKA/CREB pathway in rat hepatic stellate cells. *Int Immunopharmacol* 2015; **25**: 340-352 [PMID: 25701503 DOI: 10.1016/j.intimp.2015.02.012]

30   **Wu T**, Chen JM, Xiao TG, Shu XB, Xu HC, Yang LL, Xing LJ, Zheng PY, Ji G. Qinggan Huoxue Recipe suppresses epithelial-to-mesenchymal transition in alcoholic liver fibrosis through TGF-β1/Smad signaling pathway. *World J Gastroenterol* 2016; **22**: 4695-4706 [PMID: 27217701 DOI: 10.3748/wjg.v22.i19.4695]

31   **Tang LX**, He RH, Yang G, Tan JJ, Zhou L, Meng XM, Huang XR, Lan HY. Asiatic acid inhibits liver fibrosis by blocking TGF-beta/Smad signaling in vivo and in vitro. *PLoS One* 2012; **7**: e31350 [PMID: 22363627 DOI: 10.1371/journal.pone.0031350]

32   **Zhou DJ**, Mu D, Jiang MD, Zheng SM, Zhang Y, He S, Weng M, Zeng WZ. Hepatoprotective effect of juglone on dimethylnitrosamine-induced liver fibrosis and its effect on hepatic antioxidant defence and the expression levels of α-SMA and collagen III. *Mol Med Rep* 2015; **12**: 4095-4102 [PMID: 26126609 DOI: 10.3892/mmr.2015.3992]

33   **Zakaria S**, Youssef M, Moussa M, Akl M, El-Ahwany E, El-Raziky M, Mostafa O, Helmy AH, El-Hindawi A. Value of α-smooth muscle actin and glial fibrillary acidic protein in predicting early hepatic fibrosis in chronic hepatitis C virus infection. *Arch Med Sci* 2010; **6**: 356-365 [PMID: 22371771 DOI: 10.5114/aoms.2010.14255]

34   **Wu K**, Huang R, Wu H, Liu Y, Yang C, Cao S, Hou X, Chen B, DaI J, Wu C. Collagen-binding vascular endothelial growth factor attenuates CCl4-induced liver fibrosis in mice. *Mol Med Rep* 2016; **14**: 4680-4686 [PMID: 27748931 DOI: 10.3892/mmr.2016.5826]

35   **Fuchs BC**, Wang H, Yang Y, Wei L, Polasek M, Schühle DT, Lauwers GY, Parkar A, Sinskey AJ, Tanabe KK, Caravan P. Molecular MRI of collagen to diagnose and stage liver fibrosis. *J Hepatol* 2013; **59**: 992-998 [PMID: 23838178 DOI: 10.1016/j.jhep.2013.06.026]

36   **Cong M**, Liu T, Wang P, Fan X, Yang A, Bai Y, Peng Z, Wu P, Tong X, Chen J, Li H, Cong R, Tang S, Wang B, Jia J, You H. Antifibrotic effects of a recombinant adeno-associated virus

carrying small interfering RNA targeting TIMP-1 in rat liver fibrosis. *Am J Pathol* 2013; **182**: 1607-1616 [PMID: 23474083 DOI: 10.1016/j.ajpath.2013.01.036]

37   **Peng WH**, Tien YC, Huang CY, Huang TH, Liao JC, Kuo CL, Lin YC. Fraxinus rhynchophylla ethanol extract attenuates carbon tetrachloride-induced liver fibrosis in rats via down-regulating the expressions of uPA, MMP-2, MMP-9 and TIMP-1. *J Ethnopharmacol* 2010; **127**: 606-613 [PMID: 20035854 DOI: 10.1016/j.jep.2009.12.016]

38   **Latronico T**, Mascia C, Pati I, Zuccala P, Mengoni F, Marocco R, Tieghi T, Belvisi V, Lichtner M, Vullo V, Mastroianni CM, Liuzzi GM. Liver Fibrosis in HCV Monoinfected and HIV/HCV Coinfected Patients: Dysregulation of Matrix Metalloproteinases (MMPs) and Their Tissue Inhibitors TIMPs and Effect of HCV Protease Inhibitors. *Int J Mol Sci* 2016; **17**: 455 [PMID: 27023536 DOI: 10.3390/ijms17040455]

Baishideng®